ACS chemical biology

pubs.acs.org/acschemicalbiology

Articles

Deposition Bias of Chromatin Proteins Inverts under DNA Replication Stress Conditions

Martijn R. H. Zwinderman, Thamar Jessurun Lobo, Petra E. van der Wouden, Diana C. J. Spierings, Marcel A. T. M. van Vugt, Peter M. Lansdorp, Victor Guryev, and Frank J. Dekker*

Cite This: *ACS Chem. Biol.* 2021, 16, 2193–2201

Read Online

ACCESS | Metrics & More | Article Recommendations | Supporting Information

ABSTRACT: Following DNA replication, equal amounts of chromatin proteins are distributed over sister chromatids by re-deposition of parental chromatin proteins and deposition of newly synthesized chromatin proteins. Molecular mechanisms balancing the allocation of new and old chromatin proteins remain largely unknown. Here, we studied the genome-wide distribution of new chromatin proteins relative to parental DNA template strands and replication initiation zones using the double-click-seq. Under control conditions, new chromatin proteins were preferentially found on DNA replicated by the lagging strand machinery. Strikingly, replication stress induced by hydroxyurea or curaxin treatment and inhibition of ataxia telangiectasia and Rad3-related protein (ATR) or p53 inactivation inverted the observed chromatin protein deposition bias to the strand replicated by the leading strand polymerase in line with previously reported effects on replication protein A occupancy. We propose that asymmetric deposition of newly synthesized chromatin proteins onto sister chromatids reflects differences in the processivity of leading and lagging strand synthesis.

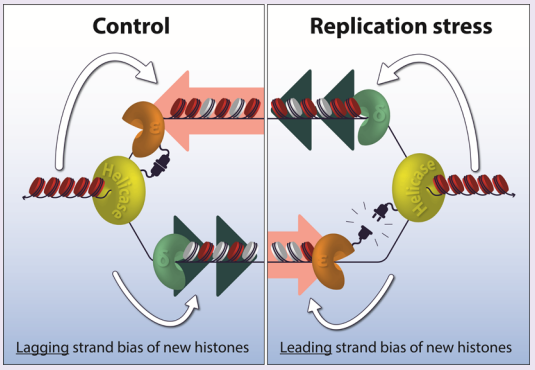

INTRODUCTION

Post-translational modifications (PTMs) of histones play important roles in the regulation of nuclear organization and gene transcription.[1] Histone PTMs are relatively stable and heritable during DNA replication.[2,3] Importantly, PTMs of parental histones differ from those of *de novo*-synthesized histones.[4] Therefore, near-symmetrical deposition of old and new histones during DNA replication is crucial to maintain similar chromatin states for the two sister chromatids following cell division. The functional importance of balanced histone inheritance was underscored by the observation that repressed chromatin domains are preserved by local re-deposition of parental histones.[5] Clearly, mechanisms for accurate deposition of parental and new histones following DNA replication are crucial.[6]

Recent studies have provided insight into histone deposition during DNA replication by using immunoprecipitation of PTMs on histones that are characteristic for either parental histones (H4K20me2) or new histones (H4K5ac).[7,8] When this approach was combined with labeling of new DNA using the thymidine analogue 5-ethynyl-2′-deoxyuridine (EdU) to separate parental from newly synthesized DNA, a slight deposition bias of new histones to the lagging strand during DNA replication was revealed in mouse embryonic stem cells.[7] A similar method was applied to budding yeast cells treated with hydroxyurea (HU), which revealed a slight bias of new histone deposition onto the leading strand.[8] A clear explanation for these opposing findings has not been reported. Of note, both studies concluded that the structural integrity of the replisome is essential to maintain near-symmetrical histone inheritance.

The structural integrity of the replication fork machinery is often compromised in cancer due to replication stress.[9] Experimentally, replication stress can be induced by inhibition of the enzyme ribonucleotide reductase (RNR) with HU.[10,11] RNR inhibition results in a reduction of nucleotides required for DNA synthesis[12] and leads to uncoupling of the replicative helicase from the leading strand DNA polymerase.[13] Helicase–polymerase uncoupling activates a DNA damage response (DDR), which involves the cell cycle checkpoint kinase ataxia telangiectasia and Rad3-related protein (ATR)[14,15] and p53-dependent transcriptional effects.[16] However, the connection between replication stress and DDR pathways in relation to histone distribution following DNA replication is largely unexplored.

Received: April 30, 2021
Accepted: September 22, 2021
Published: October 1, 2021

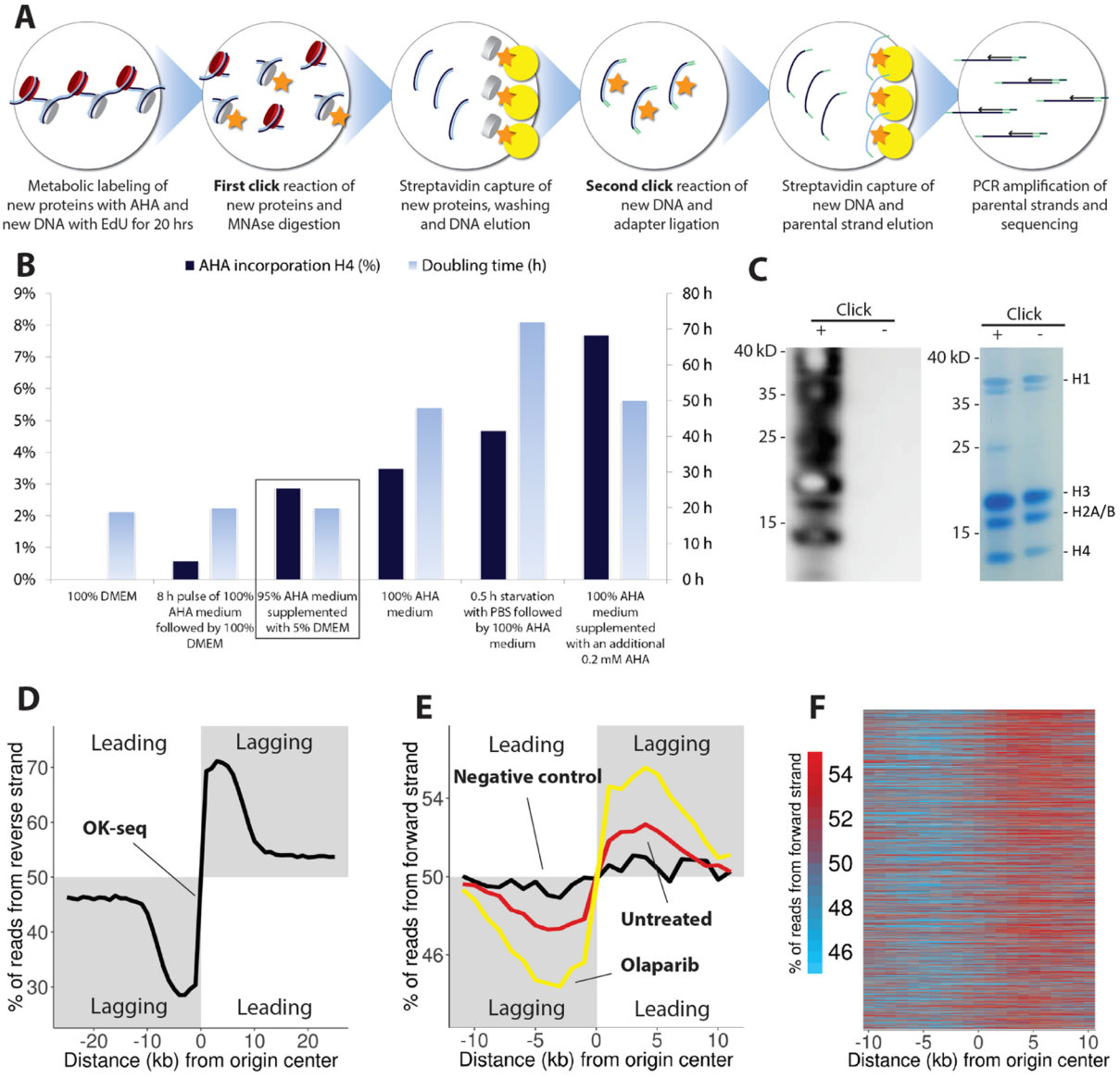

Figure 1. Double-click-seq reveals a bias in the deposition of new chromatin proteins toward the DNA strand replicated by lagging strand machinery. (A) Schematic overview of the double-click-sequencing method. (B) Effect of different culture methods on cell doubling time and the extent of AHA incorporation in histone H4 determined by mass spectrometry. Culturing hRPE-1 in 95% AHA medium supplemented with 5% DMEM for 20 h resulted in 3% AHA incorporation in histone H4 without a significant impact on cell doubling times (black box). (C) Western blot and gel electrophoresis analysis of labeled and unlabeled histones. Reactions were performed on nuclei with or without the click reaction as indicated above. Positions of histones are indicated to the right of the blot. (D) Average RFD at replication initiation zones. A plot including confidence intervals can be found in Supporting Information Figure S1B. (E) Average bias of new histone deposition at replication initiation zones under the untreated condition (red line) and with olaparib treatment (yellow line). The black line shows the background signal in hRPE-1 cells (negative control and without second click reaction). Separate plots of individual replicates including confidence intervals can be found in Supporting Information Figure S2. (F) Heatmap of new histone deposition bias at replication initiation zones under the untreated condition.

In this study, we have developed the double-click-seq protocol to enrich parental DNA bound to new chromatin proteins. In contrast to previous methods involving immunoprecipitation of histone PTMs, this approach is based on metabolic labeling of new chromatin proteins (Figure 1A). The double-click-seq provides stable labeling of *de novo* synthesized chromatin proteins by co-translational incorporation of the methionine surrogate azidohomoalanine (AHA), which allows enrichment of nucleosomes that contain new chromatin proteins following a click reaction with a biotin affinity tag. Using this methodology, we show that both replication stress as induced by HU and inhibition of the DDR invert the generally asymmetric distribution of new chromatin proteins onto replicated DNA strands in human cells. We propose that asymmetric deposition of newly synthesized chromatin proteins onto sister chromatids reflects differences in the processivity of leading and lagging strand synthesis.

RESULTS

Double-Click-Seq Reveals that Bias of New Chromatin Proteins is Skewed toward the Lagging Strand. We used immortalized human retinal pigment epithelial (hRPE-1) cells to study chromatin protein deposition onto replicated DNA. The hRPE-1 cell line has a well-characterized genome

https://doi.org/10.1021/acschembio.1c00321
ACS Chem. Biol. 2021, 16, 2193−2201

and serves as a near-diploid model of normal human cells. The initial step for development of the double-click-seq protocol was optimization of the conditions for co-translational incorporation of AHA as a replacement of methionine into newly synthesized methionine-containing proteins over the time of one replication cycle in hRPE-1. We aimed to find conditions with a minimal effect on the average cell doubling time.[17] Cells were cultured under conditions with various AHA and methionine concentrations, and histones were extracted and analyzed with mass spectrometry in order to assess the levels of AHA incorporation. Conditions were identified in which cells were cultured in a medium containing a mixture of 95% AHA and 5% methionine for 20 h to reach a 3% AHA incorporation in histone H4 (Figure 1B), which were subsequently used throughout the study. The 20 h labeling period allowed us to track histone deposition across a full cell cycle. Western blot analysis showed that AHA was also incorporated into histones H2A/B and H3 (Figure 1C).

After AHA labeling of *de novo* synthesized proteins, nuclei were isolated to remove cytoplasmic AHA-labeled proteins. The nuclei were then exposed to an initial copper-catalyzed [3 + 2] cycloaddition reaction between the azide group of AHA and an alkyne linked to biotin (click), which enabled affinity enrichment of AHA-labeled histones in complex with DNA (*i.e.*, nucleosomes) and other AHA-labeled proteins using streptavidin beads after MNAse digestion. Subsequently, several washing steps were performed to rid all DNA not bound to chromatin proteins. The remaining nucleosomal DNA was then extracted from the enriched nascent nucleosomes by digestion of chromatin proteins and streptavidin by proteinase K treatment, after which the resulting enriched DNA was ligated to forked adaptors. In a second click reaction, nascent DNA strands labeled with EdU[7] were coupled to an azide-linked biotin, thus enabling a second streptavidin bead capture. Finally, the unlabeled parental single stranded DNA was eluted from the beads with an alkaline solution and amplified to construct a directional short read sequencing library. The library was then sequenced with next generation sequencing and the resulting paired-end data (summary of all libraries in Table S1) were processed to assign genome-wide deposition of new chromatin proteins to either the forward or the reverse strand around the center of replication initiation zones (termed "origin centers" in all related figures). Autosomal replication initiation zones were mapped using a publicly available Okazaki-fragment sequencing (OK-seq) data set for hRPE-1 cells[18] (n = 9,608; Figure 1D and Supporting Information Figure S1A).

The double-click-seq revealed that the deposition bias of new chromatin proteins was skewed toward the strand replicated by the lagging strand machinery at mapped replication initiation zones (Figure 1E, red line and Figure 1F). This finding is in agreement with the bias observed in mouse embryonic stem cells.[7] However, our experiments indicate a more pronounced partition score as a measure of chromatin protein deposition bias of around 0.05 (calculated as the proportion of forward and reverse read counts, see Figure S1C), whereas Petryk *et al.* reported a partition score of approximately 0.008 for differential histone PTMs. As we observe an average replication fork directionality (RFD) of 0.42 (Supporting Information Figure S1D) where Petryk *et al.* report an average RFD of around 0.13, variability in the replication initiation zone firing rate between the different cell types used for both experiments can only partially explain the sixfold less pronounced asymmetry observed through immunoprecipitation of distinctive PTMs.[7] The remaining difference might be the result of signal dilution through the exchange of histone PTMs over time, while our method stably labels new chromatin proteins. Nonetheless, with the double-click-seq, we observed a clear bias of new chromatin proteins around replication initiation zones toward the strand replicated by lagging strand polymerases. It is worth noting that our estimate of deposition bias might be conservative since turnover times range from fast for histones H2A/H2B to slow for H4 (0.4% per hour).[6]

We hypothesized that the deposition bias of new chromatin proteins toward the lagging strand is most likely the result of the relatively less efficient capture of parental chromatin proteins by the lagging strand, thus leaving the lagging strand with more new chromatin proteins compared to the leading strand. Consequently, interfering with lagging strand synthesis would result in a more pronounced deposition bias of new chromatin proteins toward the lagging DNA strand. During lagging strand synthesis, the 5′ flap of Okazaki fragments is excised by the nuclease FEN1, upon which the fragments are ligated by DNA ligase I (LIG1).[19] Under untreated conditions, a fraction of Okazaki fragments escape LIG1-mediated ligation and are processed by a poly(ADP-ribose) polymerase (PARP)-mediated back-up route.[20] Thus, inhibition of PARP activity interferes with the completion of lagging strand synthesis. In line with our hypothesis, we observed that treatment with the PARP inhibitor olaparib[21] increased the deposition bias of new chromatin proteins onto the DNA strand replicated by lagging strand machinery (Figure 1E, yellow line). This indicates that disturbance of lagging strand synthesis increases the deposition bias of new chromatin proteins to the lagging strand compared to the untreated condition.

Replication Stress Inverts the General Asymmetric Deposition of New Chromatin Proteins. Given the observed increase in the deposition asymmetry of new chromatin proteins toward the lagging strand upon interference with lagging strand synthesis, we wondered what the effect of more general replication stress on new chromatin protein deposition would be. Strikingly, HU-induced replication stress completely inverted the bias of new chromatin proteins toward the DNA strand replicated by leading strand synthesis (Figure 2A). An inversion of the deposition bias of new chromatin proteins to the leading strand was also found upon treatment with the DNA intercalator curaxin (Figure 2B), which induces replication stress by triggering nucleosome unfolding.[22] We checked if changes in origin usage may underlie the inverted chromatin protein deposition bias; however, we found that the OK-seq profiles between untreated samples and HU treatment were highly correlated (Spearman correlation 0.98). Therefore, we conclude that replication stress, such as that induced by either HU or curaxin treatment, inverts the asymmetry in new chromatin protein deposition relative to the untreated samples. Analogously, the presence or absence of HU may explain the apparent contradiction between the leading strand bias of new histones found by Yu *et al.*[8] and the lagging strand bias of new histones found by Petryk *et al.*[7]

Inhibition of DDR Pathways Also Inverts New Chromatin Protein Deposition Asymmetry. As replication stress can lead to activation of the DDR, we speculated that the effect of replication stress on the deposition bias of new chromatin proteins might be increased by inhibition of the

https://doi.org/10.1021/acschembio.1c00321
ACS Chem. Biol. 2021, 16, 2193−2201

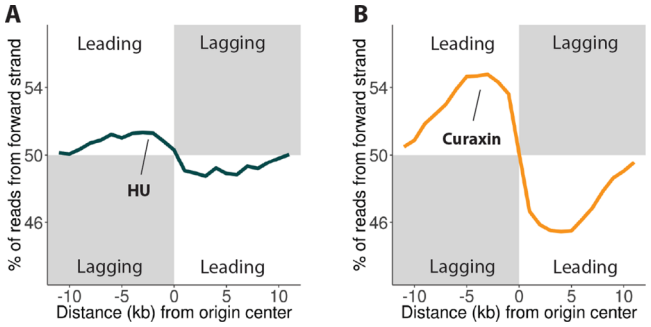

Figure 2. Replication stress inverts the deposition asymmetry of new chromatin proteins. (A) Average bias of new chromatin protein deposition at replication initiation zones during replication stress induced with HU. (B) Average bias of new chromatin protein deposition at replication initiation zones during replication stress induced with curaxin. Separate plots for individual replicates including confidence intervals can be found in Supporting Information Figure S2.

DDR. The ATR DDR pathway plays an essential role in suppressing replication stress.[15] Additional DDR pathways involve the tumor suppressor p53.[16] We therefore investigated the involvement of the ATR- and p53-mediated DDR pathways in the altered chromatin protein deposition pattern during replication stress. Toward this aim, we employed p53-null hRPE-1 cells. Lack of p53 expression was confirmed by Western blot analysis (Figure 3A). In untreated p53-null cells, a deposition bias of new histones to the leading strand was observed (Figure 3B), indicating that loss of p53 already inverts the deposition bias of new histones seen in untreated hRPE-1 cells. The bias inversion increased further upon HU treatment of the p53-null cells (Figure 3B). Pharmacological inhibition of ATR in hRPE-1 cells also led to inversion of the deposition bias of new histones toward the leading strand. Again, HU treatment provided a stronger inversion of the deposition bias of new chromatin proteins (Figure 3C). As an example, we included the heatmap of the deposition bias of new chromatin proteins in cells treated with the ATR inhibitor and HU, showing that chromatin protein bias inversion was observed consistently at the replication initiation zones that were identified (Figure 3D). We conclude that both replication stress and inhibition of DDR pathways through ATR or p53 inactivation disturb the asymmetry in the deposition of new histones such that the bias is inverted from the lagging to the leading strand.

Deposition Bias of New Chromatin Proteins Is More Pronounced in AT-Rich Regions. Finally, we investigated whether the chromatin protein deposition bias depends on common characteristics of genomic regions. We categorized replication initiation zones into actively transcribed (active) or not actively transcribed (inactive) (Figure 4C), early replicated or late replicated (Figure 4F), and AT-rich or GC-rich zones (Figure 4I). We then determined the average deposition bias of new chromatin proteins around each category of initiation zones for both untreated hRPE-1 cells ("untreated", Figure 4A,D,G) and cells treated with the ATR inhibitor and HU ("replication stress", Figure 4B,E,H). We conclude that the deposition bias tends to be stronger in late-replicated and AT-rich zones. Slight differences between replication initiation zones (Figure 4C,F,I) were observed too, but these differences were not large enough to account for the observed differences in chromatin protein deposition bias (Figure 4A,B).

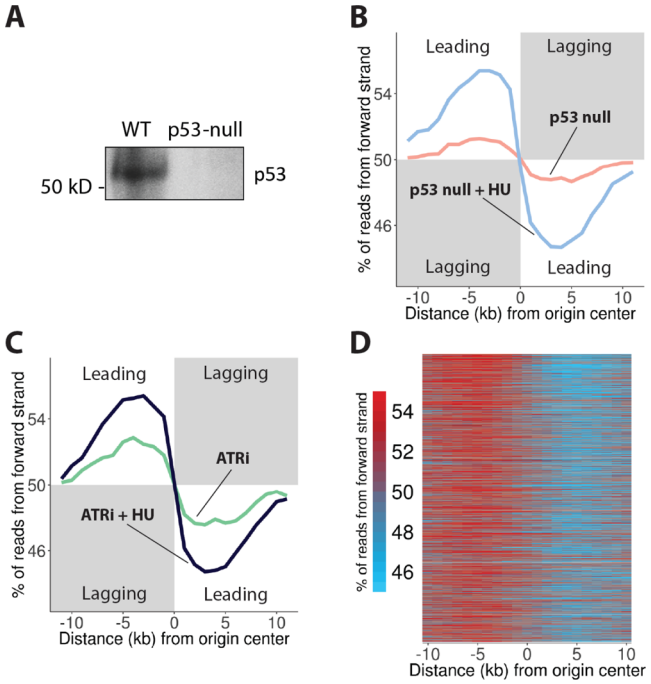

Figure 3. Inhibition of DDR pathways also inverts the deposition asymmetry of new chromatin proteins (A). Western blot showing knock-out of p53 in hRPE-1 cells with gene editing. Equal protein loading was ensured by measuring the protein concentration with the Bradford assay. (B) Average bias of new histone deposition in p53-null hRPE-1 cells treated with HU (light blue line) and without (pink line) at replication initiation zones. (C) Average bias of new histone deposition at replication initiation zones in hRPE-1 cells with either ataxia telangiectasia and Rad3-related protein (ATR) inhibition (green line) or ATR inhibition and HU treatment (dark blue line). (D) Heatmap of bias of new histone deposition at replication initiation zones in cells treated with the ATR inhibitor and HU. Separate bias plots of individual replicates including confidence intervals can be found in Supporting Information Figure S2.

Genes that are actively transcribed are generally replicated in the early S phase[23] and DNA regions replicated in the early S phase generally have higher GC-content.[24] In order to estimate the relative contribution of these genomic features to histone deposition asymmetry, we performed a multiple regression analysis taking all three factors into account (Table S2). The GC-content proved to be the most consistently significant predictor of histone deposition bias. It was significant (uncorrected p-value < 0.01) for all used conditions, with the exception of the p53 knock-out cells. The GC-content beta values indeed signified a bias increasing effect in AT-rich zones across all conditions. Replication timing was a significant predictor for the bias in cells treated with the ATR inhibitor, p53 knock-out cells, and for one out of two replicates for cells treated with curaxin and cells treated with both the ATR inhibitor and HU. Transcriptional status did not have a significant effect on the deposition bias of new chromatin proteins (Table S2).

DISCUSSION

We developed the double-click-seq method to study the incorporation of new chromatin proteins into nascent chromatin. We tracked *de novo* synthesized chromatin proteins in cultured human cells and showed that they are enriched under untreated conditions in DNA replicated by the lagging

https://doi.org/10.1021/acschembio.1c00321
ACS Chem. Biol. 2021, 16, 2193−2201

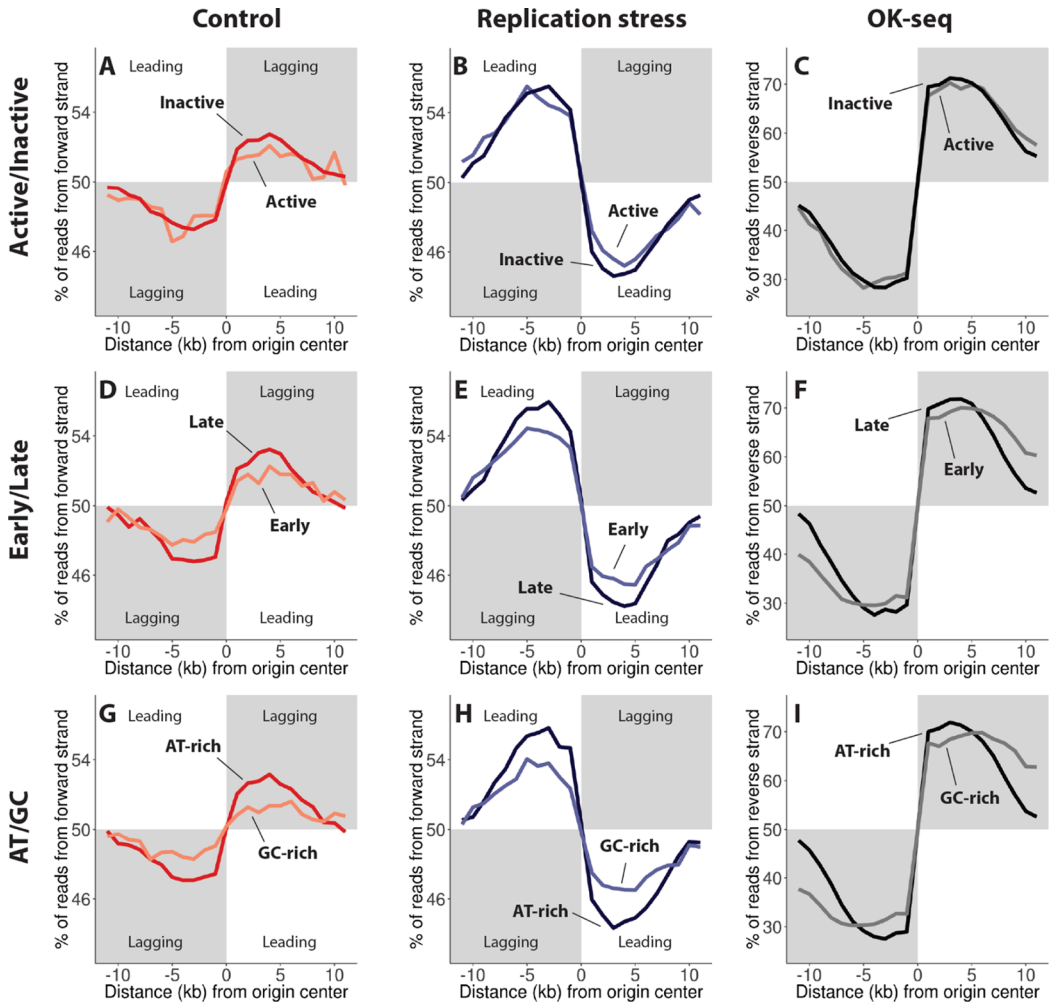

Figure 4. Deposition bias of new chromatin proteins is more pronounced in AT-rich regions. (A,D,G) Average bias of new chromatin protein deposition at replication initiation zones under untreated conditions. (B,E,H) Average bias of new chromatin protein deposition at replication initiation zones with ataxia telangiectasia and Rad3-related protein (ATR) inhibition and HU treatment. (C,F,I) Average RFD at replication initiation zones. For (A,B,C), the replication initiation zones were categorized into actively transcribed (red) and not actively transcribed (orange) regions. For (D,E,F), the zones were categorized into actively transcribed (light blue) and not actively transcribed (dark blue) regions. For (G,H,I), the zones were categorized into AT-rich (black) and GC-rich (gray) regions. Separate plots of individual replicates split into quartiles and including confidence intervals can be found in Supporting Information Figure S3.

strand machinery, especially in AT-rich regions. We found a more pronounced lagging strand bias in the deposition of new chromatin proteins than reported previously[7] and we found this to be the case around all mapped replication initiation zones.

Most likely, redistribution of parental chromatin proteins onto the DNA strand replicated by either leading or lagging strand polymerases favors the DNA strand that finishes replication first. The leading strand polymerase replicates DNA in a continuous fashion and directly follows unwinding of the parental DNA strands by the replicative helicase, such that the leading strand has the highest chance to capture a majority of the parental chromatin proteins that are evicted ahead of the replication fork. The discontinuously replicated lagging strand by default would receive a majority of new chromatin proteins to fill the gaps between re-deposited parental chromatin proteins. In support of this model, we show that interfering with the completion of lagging strand synthesis with the PARP inhibitor olaparib increases the asymmetry in new chromatin protein deposition toward the lagging strand. Thus, with olaparib, the replicated lagging strand becomes less able to capture displaced parental histones and receives even more new histones than would normally be the case.

The asymmetry of new chromatin protein deposition toward the lagging strand underwent a striking inversion toward the leading strand upon treatment with the replication stress inducers HU and curaxin. Replication stress is known to induce uncoupling between the helicase and the leading strand polymerase, which leads to single-stranded DNA (ssDNA) that requires stabilization by binding of replication protein A (RPA).[25] Interestingly, the asymmetry in RPA occupancy, as an indirect measure of ssDNA, toward the lagging strand has been found to invert upon replication stress.[25] Similarly, another study has shown that replication stress induces strand switching of the DNA clamp Proliferating Cell Nuclear Antigen (PCNA), such that more PCNA is found on the leading strand under stress conditions compared to untreated conditions.[26] Both observations indicate that replication stress increases the proportion of ssDNA on the leading strand to a greater extent than on the lagging strand. The independently operating lagging strand polymerase is apparently better equipped to handle replication stress than its leading strand

https://doi.org/10.1021/acschembio.1c00321
ACS Chem. Biol. 2021, 16, 2193−2201

counterpart, perhaps in part due to repeated relocation of the lagging strand polymerase following completion of an Okazaki fragment.[27] Therefore, when replication stressors target the replisome as a whole, the lagging strand polymerase is able to continue synthesis more effectively than the uncoupled leading strand polymerase, which is reflected in the bias inversions of RPA, PCNA, and new histones. Notably, RPA at the ssDNA is an important activator for ATRIP-ATR signaling,[28,29] involving multiple downstream effects, including on chromatin composition,[30] and could explain local differences in histone deposition. In essence, the DNA strand that is replicated by the lagging strand polymerase "leads" during replication stress.

Accumulation of RPA on the leading strand following replication stress-induced helicase-polymerase uncoupling triggers a DDR that attempts to resolve the aberrant fork structure.[13] Clearly, the DDR does not prevent inversion of new chromatin protein deposition asymmetry upon treatment with HU or curaxin. Previously, it has been demonstrated that chronic treatment of chicken DT40 cells with a low-dose of HU for 7 days stochastically induced a reduction in the expression of certain active genes, which was connected to a loss of the chromatin marks H3K4me3 and H3K9/14ac.[11] It was postulated that the observed loss of histone marks was the result of uncoupling of histone recycling from DNA synthesis due to replication stress-induced helicase−polymerase uncoupling. Our results provide more direct evidence for this hypothesis. Moreover, the results of Papadopoulou *et al.* illustrate that asymmetric deposition of new histones may accumulate over multiple cell divisions and cause epigenetic instability.[11]

Additionally, we observed that functional DDR pathways are important in maintaining the characteristic pattern of chromatin protein deposition since pharmacological inhibition of ATR and p53 knockout inverted the histone deposition pattern already without HU-induced replication stress. ATR is constitutively active in the S phase to sense ongoing DNA replication and repress FOXM1 activity.[31] After completion of the S phase, a drop in ATR activity releases the brakes on FOXM1 activity and allows cells to enter mitosis. Apparently, inhibiting this intrinsic S/G_2 checkpoint alters asymmetric histone deposition. Similarly, inactivation of *TP53* not only potentiated the observed bias inversion of new chromatin proteins in HU-induced replication stress but also caused inversion by itself. This alludes to a constitutive function of p53 in maintaining replication fork integrity.

While OK-seq profiles for hRPE-1 cells treated with HU for 3 h or without HU were strongly correlated, we did not determine the effect of a 20 h treatment with HU, the ATR inhibitor, olaparib, or p53 knock-out on OK-seq profiles. We can therefore not exclude the possibility that longer HU treatment and/or other treatments result in firing of more dormant origins, causing the asymmetry to seem weaker than it truly is. Additionally, some secondary cell divisions cannot be excluded because of the long labeling time. Such events might again weaken the asymmetry signal but not enhance it or change its direction.

Furthermore, we observe that chromatin protein deposition asymmetry is increased close to replication initiation zones located in AT-rich DNA. AT-rich DNA is less stable than GC-rich DNA due to a difference in hydrogen bonding.[32] This difference in DNA stability leads to a higher rate of DNA unwinding in AT-rich compared to GC-rich regions, not taking the chromatic context into account.[33] Such an increase in DNA unwinding rate may increase leading strand synthesis speed in untreated conditions and helicase−polymerase uncoupling during replication stress. In both cases, this would lead to a greater difference in leading and lagging strand processivity in AT-rich compared to GC-rich regions and thus result in an increase in the asymmetry of new chromatin protein deposition.

We note that EdU labeling affects the cell cycle by an increase of the G2/M phase (Supporting Information Figure S4) in line with literature describing that EdU delays the cell cycle but does not affect the rate of elongation of replication forks during synthesis.[34] Since application of EdU is currently the only technology to separate new and old DNA, it is not possible to include a control experiment for the effect of EdU itself. This demonstrates, on one hand, the need for a Blanc experiment as a reference for further experimental variation (Figure 1E, black line) and, on the other hand, the need to advance this type of technology further to enable analysis of histone deposition bias under less perturbing conditions.

In our hands, metabolic labeling of new histones with AHA is limited to approximately 3% of cellular histone H4 over the course of a 20 h incubation period. All histone isoforms contain a methionine that can be replaced by AHA during *de novo* synthesis. Therefore, a labeling period that covers a full cell cycle leads to AHA incorporation in histones H3.3 and H2A/B, which have a replication-independent turnover.[35] Histone H4 may also turnover independently from replication, but this seems mostly confined to centromeric regions.[36] Regardless, replication-independent turnover of histones could decrease the chromatin protein deposition asymmetry but not enhance it or change its direction. Also, we considered the possibility that the asymmetric distribution of newly synthesized proteins onto replicated DNA could reflect other proteins than histones, for example, proteins that transiently associate with DNA during replication such as RPA and PCNA. We dismissed this possibility because (1) histones are by far the most abundant proteins associated with DNA at any time, (2) in our double-click-seq method, we sequence DNA typically long after replication (by pulling down recently synthesized proteins and sequencing associated parental DNA template strands), and (3) we enrich for DNA fragments <200 bp and exclude fragments with size <145 bp from analysis. We also considered the fact that some old and newly synthesized histones will be exchanged after DNA replication before being pulled down in our method. Such post replication histone exchange events are expected to diminish the observed asymmetry in the distribution of new *versus* old chromatin proteins over DNA replicated by leading *versus* lagging strand synthesis. Inversion of this asymmetry upon replication stress is furthermore difficult to reconcile with histone exchanges after DNA replication. For a more general analysis of strand-specific protein binding at replication forks, we refer to the eSPAN method.[26]

In conclusion, our observations indicate that the deposition of newly synthesized proteins onto nascent chromatin is inherently biased toward the lagging strand and that this bias increases upon PARP inhibition. Replication stress induced by HU or curaxin, genetic inactivation of p53, or pharmacological ATR kinase inhibition inverts the deposition bias of new chromatin toward the leading strand. These findings can be united by a model that includes differences in processivity of leading and lagging strand synthesis. Normally, polymerase ε on the leading strand is tightly coupled to the replicative

https://doi.org/10.1021/acschembio.1c00321
ACS Chem. Biol. 2021, 16, 2193−2201

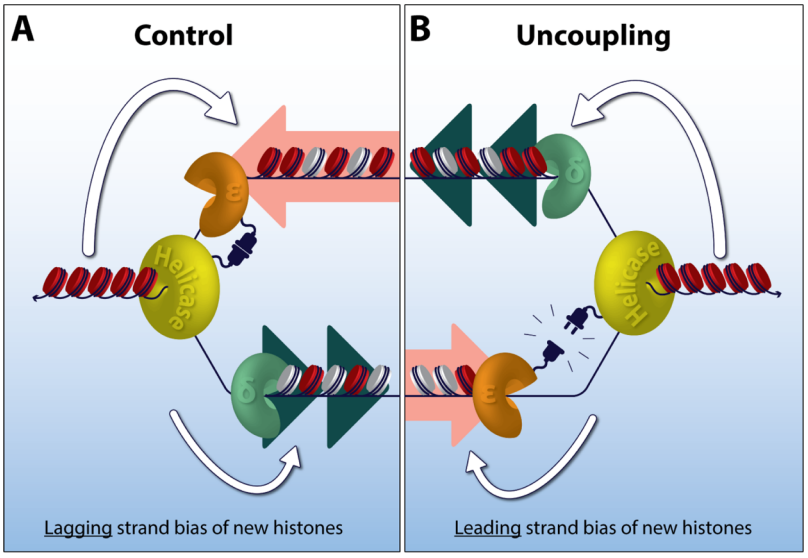

Figure 5. Helicase–polymerase uncoupling during replication stress inverts deposition of chromatin proteins exemplified by histones. (A) Model of lagging strand (green arrow heads) bias of new histones (white spheres) under untreated conditions following the leading strand (pink arrow) bias of old histones (red spheres), with polymerase ε (orange) coupled to the helicase (yellow). (B) Model of leading strand bias of new histone deposition following helicase uncoupling of polymerase ε. Helicase uncoupling results in lagging of leading strand synthesis. This results in a leading strand bias for new histones resulting from a biased re-deposition of old histones onto the faster completed lagging strand.

helicase, whereas polymerase δ on the lagging strand is operating independently.[37] As a result, re-deposition of parental chromatin is biased toward the faster completed leading strand and deposition of new chromatin is biased toward the lagging strand (Figure 5A). Helicase–polymerase uncoupling, due to a lack of polymerase ε processivity during replication stress, results in stretches of ssDNA on the leading strand.[37,38] The independently operating polymerase δ maintains processivity and therefore completes replication faster than polymerase ε.[38] Together, this results in increased re-deposition of parental chromatin proteins and decreased deposition of new chromatin proteins on DNA replicated by polymerase δ, thus explaining the inversion of new chromating protein deposition asymmetry toward the strand replicated by polymerase ε during replication stress (Figure 5B).

DATA AVAILABILITY

The data sets generated during this study are available at EBI ArrayExpress under accession number E-MTAB-8624. The code generated during this study is available at GitHub; https://github.com/thamarlobo/histone_deposition_analysis.git.

ASSOCIATED CONTENT

Supporting Information

The Supporting Information is available free of charge at https://pubs.acs.org/doi/10.1021/acschembio.1c00321.

Additional information on materials and methods; heatmap of replication fork directionality at replication initiation zones, average replication fork directionality at replication initiation zones, average bias of new histone deposition at replication initiation zones, SDS-PAGE result of washing steps of first streptavidin pull-down; deposition bias in individual replicates; histone deposition bias and replication fork direction in separate replicates for genomic clusters; and cell cycle analysis double-click-seq protocol conditions (PDF)

AUTHOR INFORMATION

Corresponding Author

Frank J. Dekker – *Department of Chemical and Pharmaceutical Biology, Groningen Research Institute of Pharmacy, University of Groningen, 9713 AV Groningen, The Netherlands;* orcid.org/0000-0001-7217-9300; Email: f.j.dekker@rug.nl

Authors

Martijn R. H. Zwinderman – *Department of Chemical and Pharmaceutical Biology, Groningen Research Institute of Pharmacy, University of Groningen, 9713 AV Groningen, The Netherlands*

Thamar Jessurun Lobo – *European Research Institute for the Biology of Ageing, University of Groningen, University Medical Center Groningen, 9713 AV Groningen, The Netherlands*

Petra E. van der Wouden – *Department of Chemical and Pharmaceutical Biology, Groningen Research Institute of Pharmacy, University of Groningen, 9713 AV Groningen, The Netherlands*

Diana C. J. Spierings – *European Research Institute for the Biology of Ageing, University of Groningen, University Medical Center Groningen, 9713 AV Groningen, The Netherlands*

Marcel A. T. M. van Vugt – *Department of Medical Oncology, University Medical Center Groningen, University of Groningen, 9713 GZ Groningen, The Netherlands*

Peter M. Lansdorp – *European Research Institute for the Biology of Ageing, University of Groningen, University Medical Center Groningen, 9713 AV Groningen, The Netherlands; Terry Fox Laboratory, British Columbia Cancer Agency, Vancouver V5Z 1L3 British Columbia, Canada; Department of Medical Genetics, University of British Columbia, Vancouver V6T 1Z4 British Columbia, Canada*

https://doi.org/10.1021/acschembio.1c00321
ACS Chem. Biol. 2021, 16, 2193–2201

Victor Guryev − *European Research Institute for the Biology of Ageing, University of Groningen, University Medical Center Groningen, 9713 AV Groningen, The Netherlands*

Complete contact information is available at: https://pubs.acs.org/10.1021/acschembio.1c00321

Author Contributions

M.R.H.Z. and T.J.L. contributed equally to this work. Conceptualization, P.M.L., F.J.D., and M.R.H.Z.; investigation, methodology, and validation, M.R.H.Z. and P.E.W. with help from D.C.J.S.; data curation, formal analysis, and software, T.J.L. and V.G.; project administration, M.R.H.Z.; funding acquisition, resources, and supervision, F.J.D., V.G., D.C.J.S, P.M.L., and M.A.T.M.V.; visualization, M.R.H.Z and T.J.L.; writing—original draft, M.R.H.Z.; writing—review & editing, all authors. P.M.L., V.G. and F.J.D. should be regarded as joint senior authors of the manuscript. F.J.D. lead contact.

Funding

F.J.D. is funded by a starting grant (Nr 309782) from the European Research Council and a VIDI grant (Nr 639.033.907) from the Netherlands Organization of Scientific Research. P.M.L. is funded by an advanced grant (Nr 294740) from the European Research Council. M.A.T.M.V. is funded by a consolidator grant (Nr 682421) from the European Research Council.

Notes

The authors declare no competing financial interest.

■ ACKNOWLEDGMENTS

We thank M. Groves for comments on the manuscript and K. Hoekstra-Wakker, J. Beenen, and N. Halsema for help with sequencing.

■ REFERENCES

(1) Allis, C. D.; Jenuwein, T. The molecular hallmarks of epigenetic control. *Nat. Rev. Genet.* **2016**, *17*, 487.

(2) Audergon, P. N. C. B.; Catania, S.; Kagansky, A.; Tong, P.; Shukla, M.; Pidoux, A. L.; Allshire, R. C. Restricted epigenetic inheritance of H3K9 methylation. *Science* **2015**, *348*, 132−135.

(3) Ragunathan, K.; Jih, G.; Moazed, D. Epigenetic inheritance uncoupled from sequence-specific recruitment. *Science* **2015**, *348*, 1258699.

(4) Reverón-Gómez, N.; González-Aguilera, C.; Stewart-Morgan, K. R.; Petryk, N.; Flury, V.; Graziano, S.; Johansen, J. V.; Jakobsen, J. S.; Alabert, C.; Groth, A. Accurate Recycling of Parental Histones Reproduces the Histone Modification Landscape during DNA Replication. *Mol. Cell* **2018**, *72*, 239−249.e5.

(5) Escobar, T. M.; Oksuz, O.; Saldaña-Meyer, R.; Descostes, N.; Bonasio, R.; Reinberg, D. Active and Repressed Chromatin Domains Exhibit Distinct Nucleosome Segregation During DNA Replication. *Cell* **2019**, *179*, 953−963.

(6) Alabert, C.; Barth, T. K.; Reverón-Gómez, N.; Sidoli, S.; Schmidt, A.; Jensen, O. N.; Imhof, A.; Groth, A. Two distinct modes for propagation of histone PTMs across the cell cycle. *Genes Dev.* **2015**, *29*, 585−590.

(7) Petryk, N.; Dalby, M.; Wenger, A.; Stromme, C. B.; Strandsby, A.; Andersson, R.; Groth, A. MCM2 promotes symmetric inheritance of modified histones during DNA replication. *Science* **2018**, *361*, 1389−1392.

(8) Yu, C.; Gan, H.; Serra-Cardona, A.; Zhang, L.; Gan, S.; Sharma, S.; Johansson, E.; Chabes, A.; Xu, R.-M.; Zhang, Z. A mechanism for preventing asymmetric histone segregation onto replicating DNA strands. *Science* **2018**, *361*, 1386−1389.

(9) Alexander, J. L.; Orr-Weaver, T. L. Replication fork instability and the consequences of fork collisions from rereplication. *Genes Dev.* **2016**, *30*, 2241−2252.

(10) Chapman, T. R.; Kinsella, T. J. Ribonucleotide reductase inhibitors: A new look at an old target for radiosensitization. *Front. Oncol.* **2012**, *1*, 56.

(11) Papadopoulou, C.; Guilbaud, G.; Schiavone, D.; Sale, J. E. Nucleotide Pool Depletion Induces G-Quadruplex-Dependent Perturbation of Gene Expression. *Cell Rep.* **2015**, *13*, 2491−2503.

(12) Koç, A.; Wheeler, L. J.; Mathews, C. K.; Merrill, G. F. Hydroxyurea Arrests DNA Replication by a Mechanism that Preserves Basal dNTP Pools. *J. Biol. Chem.* **2004**, *279*, 223−230.

(13) Byun, T. S.; Pacek, M.; Yee, M. C.; Walter, J. C.; Cimprich, K. A. Functional uncoupling of MCM helicase and DNA polymerase activities activates the ATR-dependent checkpoint. *Genes Dev.* **2005**, *19*, 1040−1052.

(14) Toledo, L. I.; Altmeyer, M.; Rask, M.-B.; Lukas, C.; Larsen, D. H.; Povlsen, L. K.; Bekker-Jensen, S.; Mailand, N.; Bartek, J.; Lukas, J. ATR prohibits replication catastrophe by preventing global exhaustion of RPA. *Cell* **2013**, *155*, 1088.

(15) Zou, L.; Elledge, S. J. Sensing DNA damage through ATRIP recognition of RPA-ssDNA complexes. *Science* **2003**, *300*, 1542−1548.

(16) Klusmann, I.; Rodewald, S.; Müller, L.; Friedrich, M.; Wienken, M.; Li, Y.; Schulz-Heddergott, R.; Dobbelstein, M. p53 Activity Results in DNA Replication Fork Processivity. *Cell Rep.* **2016**, *17*, 1845−1857.

(17) Arnaudo, A. M.; Link, A. J.; Garcia, B. A. Bioorthogonal Chemistry for the Isolation and Study of Newly Synthesized Histones and Their Modifications. *ACS Chem. Biol.* **2016**, *11*, 782−791.

(18) Chen, Y.-H.; Keegan, S.; Kahli, M.; Tonzi, P.; Fenyö, D.; Huang, T. T.; Smith, D. J. Transcription shapes DNA replication initiation and termination in human cells. *Nat. Struct. Mol. Biol.* **2019**, *26*, 67−77.

(19) Balakrishnan, L.; Bambara, R. A. Okazaki fragment metabolism. *Cold Spring Harbor Perspect. Biol.* **2013**, *5*, a010173.

(20) Hanzlikova, H.; Kalasova, I.; Demin, A. A.; Pennicott, L. E.; Cihlarova, Z.; Caldecott, K. W. The Importance of Poly(ADP-Ribose) Polymerase as a Sensor of Unligated Okazaki Fragments during DNA Replication. *Mol. Cell* **2018**, *71*, 319−331.e3.

(21) Menear, K. A.; Adcock, C.; Boulter, R.; Cockcroft, X.-l.; Copsey, L.; Cranston, A.; Dillon, K. J.; Drzewiecki, J.; Garman, S.; Gomez, S.; Javaid, H.; Kerrigan, F.; Knights, C.; Lau, A.; Loh, V. M.; Matthews, I. T. W.; Moore, S.; O'Connor, M. J.; Smith, G. C. M.; Martin, N. M. B. 4-[3-(4-Cyclopropanecarbonylpiperazine-1-carbonyl)-4-fluorobenzyl] -2H-phthalazin-1-one: A novel bioavailable inhibitor of poly(ADP-ribose) polymerase-1. *J. Med. Chem.* **2008**, *51*, 6581−6591.

(22) Safina, A.; Cheney, P.; Pal, M.; Brodsky, L.; Ivanov, A.; Kirsanov, K.; Lesovaya, E.; Naberezhnov, D.; Nesher, E.; Koman, I.; Wang, D.; Wang, J.; Yakubovskaya, M.; Winkler, D.; Gurova, K. FACT is a sensor of DNA torsional stress in eukaryotic cells. *Nucleic Acids Res.* **2017**, *45*, 1925−1945.

(23) Hatton, K. S.; Dhar, V.; Brown, E. H.; Iqbal, M. A.; Stuart, S.; Didamo, V. T.; Schildkraut, C. L. Replication program of active and inactive multigene families in mammalian cells. *Mol. Cell. Biol.* **1988**, *8*, 2149−2158.

(24) Woodfine, K.; Fiegler, H.; Beare, D. M.; Collins, J. E.; McCann, O. T.; Young, B. D.; Debernardi, S.; Mott, R.; Dunham, I.; Carter, N. P. Replication timing of the human genome. *Hum. Mol. Genet.* **2004**, *13*, 191−202.

(25) Gan, H.; Yu, C.; Devbhandari, S.; Sharma, S.; Han, J.; Chabes, A.; Remus, D.; Zhang, Z. Checkpoint Kinase Rad53 Couples Leading- and Lagging-Strand DNA Synthesis under Replication Stress. *Mol. Cell* **2017**, *68*, 446−455.e3.

(26) Yu, C.; Gan, H.; Han, J.; Zhou, Z.-X.; Jia, S.; Chabes, A.; Farrugia, G.; Ordog, T.; Zhang, Z. Strand-Specific Analysis Shows Protein Binding at Replication Forks and PCNA Unloading from Lagging Strands when Forks Stall. *Mol. Cell* **2014**, *56*, 551−563.

(27) Yu, C.; Gan, H.; Zhang, Z. Both DNA Polymerases δ and ε Contact Active and Stalled Replication Forks Differently. *Mol. Cell. Biol.* **2017**, *37*, No. e00190-17.
(28) Ball, H. L.; Myers, J. S.; Cortez, D. ATRIP binding to replication protein A-single-stranded DNA promotes ATR-ATRIP localization but is dispensable for Chk1 phosphorylation. *Mol. Biol. Cell* **2005**, *16*, 2372−2381.
(29) Zou, L.; Elledge, S. J. Sensing DNA damage through ATRIP recognition of RPA-ssDNA complexes. *Science* **2003**, *300*, 1542−1548.
(30) Matsuoka, S.; Ballif, B. A.; Smogorzewska, A.; McDonald, E. R.; Hurov, K. E.; Luo, J.; Bakalarski, C. E.; Zhao, Z.; Solimini, N.; Lerenthal, Y.; Shiloh, Y.; Gygi, S. P.; Elledge, S. J. ATM and ATR substrate analysis reveals extensive protein networks responsive to DNA damage. *Science* **2007**, *316*, 1160−1166.
(31) Saldivar, J. C.; Hamperl, S.; Bocek, M. J.; Chung, M.; Bass, T. E.; Cisneros-Soberanis, F.; Samejima, K.; Xie, L.; Paulson, J. R.; Earnshaw, W. C.; Cortez, D.; Meyer, T.; Cimprich, K. A. An intrinsic S/G2 checkpoint enforced by ATR. *Science* **2018**, *361*, 806−810.
(32) Yakovchuk, P.; Protozanova, E.; Frank-Kamenetskii, M. D. Base-stacking and base-pairing contributions into thermal stability of the DNA double helix. *Nucleic Acids Res.* **2006**, *34*, 564−574.
(33) Pandey, M.; Patel, S. S. Helicase and Polymerase Move Together Close to the Fork Junction and Copy DNA in One-Nucleotide Steps. *Cell Rep.* **2014**, *6*, 1129−1138.
(34) Kohlmeier, F.; Maya-Mendoza, A.; Jackson, D. A. EdU induces DNA damage response and cell death in mESC in culture. *Chromosome Res.* **2013**, *21*, 87−100.
(35) Deal, R. B.; Henikoff, J. G.; Henikoff, S. Genome-Wide Kinetics of Nucleosome Turnover Determined by Metabolic Labeling of Histones. *Science* **2010**, *328*, 1161−1164.
(36) Ahmad, K.; Henikoff, S. The histone variant H3.3 marks active chromatin by replication-independent nucleosome assembly. *Mol. Cell* **2002**, *9*, 1191−1200.
(37) Graham, J. E.; Marians, K. J.; Kowalczykowski, S. C. Independent and Stochastic Action of DNA Polymerases in the Replisome. *Cell* **2017**, *169*, 1201−1213.e17.
(38) Georgescu, R. E.; Yao, N.; Indiani, C.; Yurieva, O.; O'Donnell, M. E. Replisome mechanics: Lagging strand events that influence speed and processivity. *Nucleic Acids Res.* **2014**, *42*, 6497−6510.

https://doi.org/10.1021/acschembio.1c00321
ACS Chem. Biol. 2021, 16, 2193−2201